


EXPRESS LETTER

Open Access



Evolution of field-aligned current in the meridional plane during substorm: multipoint observations from satellites and ground stations

Shun Imajo^{1*} , Masahito Nosé¹, Mari Aida², Nana Higashio², Haruhisa Matsumoto², Koga Kiyokazu², Charles Smith³, Robert J. MacDowall⁴ and Akimasa Yoshikawa⁵

Abstract

We report the propagation of substorm-associated magnetic fluctuations by multipoint magnetic observations from ground and space in the same meridional plane. The first Quasi-Zenith Satellite (QZS-1), which has a unique orbit of quasi-zenith orbit with an inclination of 41° , an apogee of $7.1 R_E$ radial distance, and an orbital period of 24 h, can stay for a long time in the near-earth magnetotail away from the magnetic equator. We examined a substorm event during 15:00–16:00 UT on July 09, 2013 when QZS-1 was located at 31° dipole latitude and 23.5 h dipole magnetic local time. The Engineering Test Satellite VIII (ETS-VIII), Time History of Events and Macroscale Interactions during Substorms D (THEMIS-D) at a radial distance of $\sim 10 R_E$, and THEMIS-E at a radial distance of $\sim 7 R_E$ were located near the equator in the similar magnetic meridian. The dipolarization was first observed at THEMIS-D at 15:14:30 UT. Then, ~ 1 min later, magnetic fluctuations were observed by ETS-VIII and THEMIS-E. At the same time, the magnetic bay and Pi2 pulsation were observed at low-latitude magnetic observatories and the Radiation Belt Storm Probes B satellite in the inner magnetosphere. We found that QZS-1 away from the equator observed a strong azimuthal magnetic field fluctuation with a long delay of 15 min from the first dipolarization at THEMIS-D near the equator. The speed of the poleward propagating magnetic fluctuation between the ionospheric footprints is calculated to be 310 [m/s], which is consistent with a typical speed of auroral poleward expansion. A similar time delay of the onset of the negative bay was observed between the Tixie (AACGM MLAT = 66.8°) and Kotelny (AACGM MLAT = 71.0°) observatories near the ionospheric footprint of satellites. We suggest that the long delay time of the magnetic fluctuation at QZS-1 was associated with the crossing of field-aligned current during the poleward expansion of the substorm current system. The distribution of azimuthal magnetic field variations in the magnetosphere indicates that the east side downward current extended more west side in the higher latitude part of the current wedge.

Keywords: Substorm expansion phase, Evolution of substorm current system, Dipolarization, Latitudinal propagation in the magnetosphere, Quasi-zenith orbit

Introduction

The magnetic fluctuations associated with the substorm expansion phase reflects the structure and development

of substorm current systems. In the auroral zone, the westward electrojet drives the negative magnetic bay, which is a rapid decrease in the north–south magnetic field. The field-aligned current (FAC) connecting to the westward electrojet magnetic field creates the positive magnetic bay at middle-to-low latitudes. A typical magnetic signature in the geosynchronous orbit is a sudden

*Correspondence: imajos@isee.nagoya-u.ac.jp

¹ Institute for Space-Earth Environmental Research, Nagoya University, Nagoya, Japan

Full list of author information is available at the end of the article

increase in the magnetic field being aligned with the magnetic dipole axis, the so-called magnetic dipolarization (e.g., Cummings et al. 1968). The dipolarization magnetic signature corresponds to the disruption of the westward cross-tail currents (Lui 1996). The deflection of the east–west magnetic field is also observed with the dipolarization, which is consistent with the development of the upward and downward FACs farther than the geosynchronous altitude (Nagai 1982). The current system, which is well known as the substorm current wedge, consists of the westward electrojet in the ionosphere, upward and downward FACs, and its magnetospheric closure (see a review by Kepko et al. 2015).

The propagation of such magnetic fluctuations is important for understanding the evolution of the substorm current system. It is known that the negative bay propagates poleward during the expansion phase, indicating the poleward motion of the westward electrojet in the ionosphere (e.g., Akasofu 1960). On the other hand, in the magnetosphere, dipolarizations show both earthward and tailward propagations in the radial distance range of 4–30 R_E (Jacquey et al. 1991; Ohtani et al. 1992; Jacquey et al. 1993; Ohtani et al. 1998; Baumjohann et al. 1999; Liou et al. 2002; Ohtani et al. 2018). The observations around the geosynchronous altitude have been limited in the near equator below 20° magnetic latitude, and the latitudinal distribution of magnetic fluctuations has not been well understood. Also, it is not clear whether the propagation of the dipolarization is associated with the poleward motion of the westward electrojet because these previous studies were not included the simultaneous magnetic observations at the conjugate point on the ground.

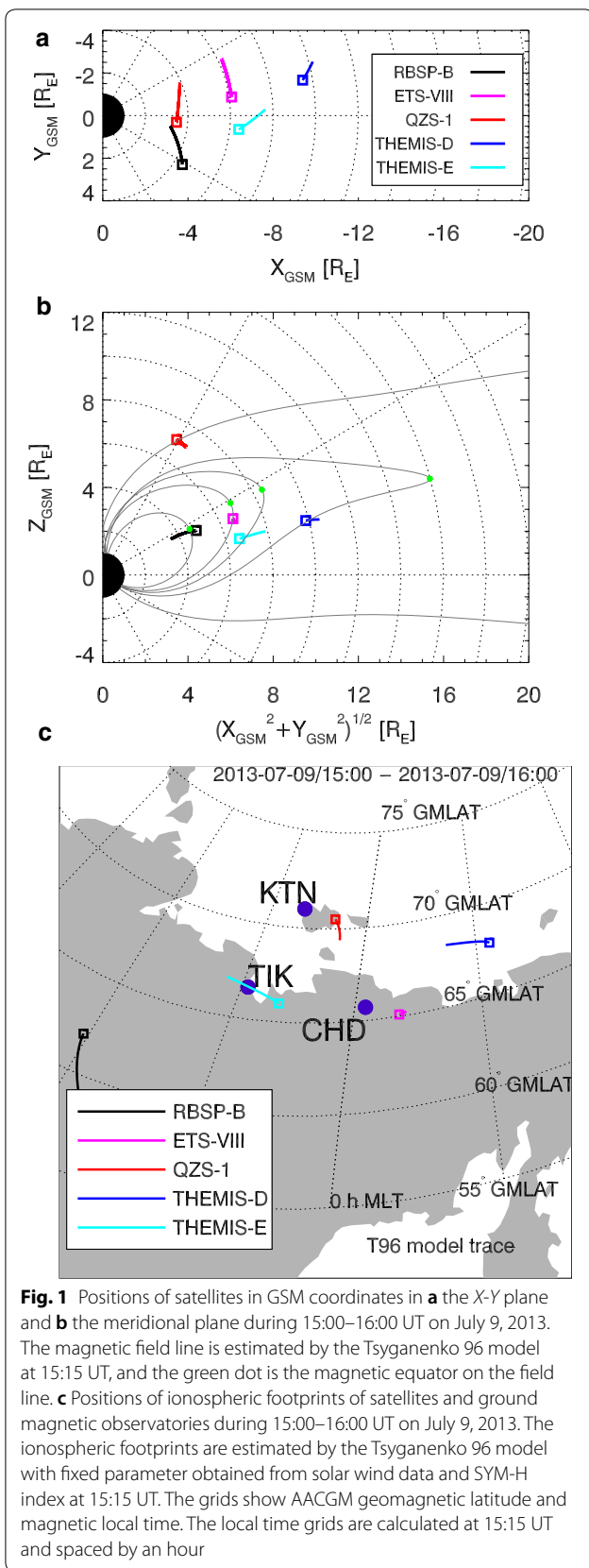
The FAC distribution in the ionosphere and its temporal evolution during substorms have been extensively studied by ground-based magnetometers and low-altitude satellites (e.g., Iijima and Potemra 1976; Kamide et al. 1996; Gjerloev and Hoffman 2002). The FAC evolution in the magnetosphere during substorms is not well understood, in particular, in the high-latitude part of the FAC. The substorm current system in the ionosphere during the expansion phase can reach the poleward boundary of the auroral oval, which may connect to the distant tail. However, it is difficult to examine the magnetospheric part of the current system using low-inclination satellites, because the trace of the magnetic field from the distant tail to the ionosphere can cause a large error in estimating the footprint location, and there are rare opportunities of conjunction observations with a satellite in the distant tail.

In this study, we examine the propagation of magnetic fluctuations in the near-earth magnetotail in the same meridional plane and its relation to ground magnetic phenomena. The main advantage of this study is simultaneous observations by near-equatorial satellites and the

first Quasi-Zenith Satellite (QZS-1) away from the magnetic equator. Since QZS-1 stays in the specific longitude around Japan, the geosynchronous satellite ETS-VIII and the ground magnetometer in Kotelnny Island near the ionospheric footprint of QZS-1 are always located in the close magnetic local time. We analyze a substorm event on July 9, 2013 during 15:00–16:00 UT when QZS-1 was located at 31° dipole magnetic latitude (MLAT) and 23.5 h dipole magnetic local time (MLT), the Radiation Belt Storm Probe B (RBSP-B) satellite was located inside the geosynchronous altitude, and Time History of Events and Macroscale Interactions during Substorms D (THEMIS-D) and THEMIS-E were located outside the geosynchronous altitude in the similar MLT of QZS-1.

Data set

Figure 1 shows the positions of satellites and ground observatories. The QZS-1 satellite, also called the Michibiki-1 satellite, has a quasi-zenith orbit with a perigee of 6.0 R_E radial distance, an apogee of 7.1 R_E radial distance, and an inclination of 41° (Ishijima et al. 2009). The QZS-1 satellite has two fluxgate magnetometers (MAM-S1 and MAM-S2) with a sampling rate of 1 s for monitoring the space environment (Furuhata et al. 2012). We used MAM-S2 data because the noise level was smaller than MAM-S1 data during the analyzed period. To observe the magnetic fluctuations near the magnetic equator, we used the magnetic data from MAM onboard the Engineering Test Satellite VIII (ETS-VIII) (Koga and Obara 2009) with a time resolution of 0.5 s, FGMs onboard THEMIS-D and THEMIS-E satellites with a time resolution of 3 s (spin resolution) (Angelopoulos et al. 2009), and EMFISIS onboard the RBSP-B satellite with a time resolution of 4 s (Kletzing et al. 2013). The offset value of QZS-1 and ETS-VIII was modified by adding constant values to the magnetic field data in each satellite coordinate. We used the same offset value of ETS-VIII estimated by the method of Nosé et al. (2014). The offset value of QZS-1 was estimated by the same method. All satellite magnetic data are transformed into the *VDH* coordinate system: the *H* axis is antiparallel to the terrestrial magnetic dipole, the *V* axis points radially outward and is parallel to the dipole equator, and *D* completes a right-handed orthogonal system and points eastward. The residual magnetic field data (ΔV , ΔD , and ΔH) were obtained by subtracting the Tsyganenko 89 model field (Tsyganenko 1989) during quiet conditions ($K_p = 0$) from observed data. ETS-VIII, THEMIS-D, THEMIS-E, and RBSP-B were located in the southern hemisphere with respect to the magnetic equator of the Tsyganenko 96 model field. A positive value of the *V* component (not shown here) also supports that these satellites were located in the southern hemisphere.



We used the ground magnetic data from observatories of MAGnetic Data Acquisition System/Circum-pacific Magnetometer Network (MAGDAS/CPMN) (Yumoto 2006, 2007). The information on the magnetic observatories is listed in Table 1. We used the high-latitude ground magnetic data from KTN near the footprint of QZS-1, TIK near the footprint of THEMIS-E, and CHD near the footprint of ETS-VIII as shown in Fig. 1c. The low-latitude magnetic field data from ASB and EWA were also used to see the magnetic bay: the integrated magnetic signature of the high-latitude FAC system (the positions are not shown in the figure).

Observations

Figure 2a–g shows magnetic field data from satellites equal to or farther than the geosynchronous altitude and high-latitude ground observatories. Figure 2h shows altitude-adjusted corrected geomagnetic (AACGM) coordinates (Baker and Wing 1989) magnetic latitude of footprints and ground observatories at 100 km in altitude as a reference. The magnetic field variation was first observed at THEMIS-D at ~ 15:14:30 UT (Fig. 2c). The ΔH component increased, and the ΔV component decreased, which are a typical signature of the magnetic dipolarization in the southern hemisphere, with superimposed oscillations. The ΔD component initially shows a small negative deflection and then a large positive deflection. About 1 min later, ETS-VIII and THEMIS-E observed a strong negative excursion of ΔD (Fig. 2a, b). This indicates the magnetic fluctuation propagated earthward in the region of 6.6–10 R_E near the magnetic equator. ETS-VIII observed the high-frequency bursts in ΔH and ΔV components of ETS-VIII at 15:17:30 and 15:24:30 UT. These high-frequency bursts at the substorm onset have been considered to be a drift-driven electromagnetic ion cyclotron wave (e.g., Lui et al. 2008), but are not discussed in this paper. The QZS-1 satellite away from the magnetic equator observed a strong negative excursion of the ΔD component at 15:29:30 UT (Fig. 2d) with a long delay of ~ 15 min from the first variation at THEMIS-D. A small positive ΔV excursion at QZS-1 may indicate field line dipolarization in the northern hemisphere. The time delay indicates that the magnetic fluctuation propagated tailward (or poleward) between THEMIS-D and QZS-1. The negative bay, which is an indicator of the ionospheric westward electrojet, shows a similar delay between the stations near the footprint of the satellites. The negative bay observed at CHD and TIK started at ~ 15 : 15 : 00 UT, almost the same timing at satellites near the magnetic equator (Fig. 2e, f). On the other hand, KTN near the footprint of QZS-1 observed a negative bay at 15:28:00 UT, which is close to but slightly earlier than the onset at QZS-1 (Fig. 2g). The ground observation near the footprint indicated that the poleward expansion of the westward electrojet was consistent with the

Table 1 The information on magnetic observatories

Station name	Station code	Geographic Latitude	Geographic Longitude	Geomagnetic Latitude	Geomagnetic Longitude
Kotelny	KTN	75.94	137.7	71.04	202.69
Tixie	TIK	71.58	128.90	66.78	198.52
Chokurdakh	CHD	70.62	147.89	65.80	213.96
Ashibetsu	ASB	43.46	142.17	37.25	214.78
Ewa beach	EWA	21.32	202.00	21.96	270.89

Geomagnetic latitude and longitude at 100 km above the observatories are defined by altitude-adjusted corrected geomagnetic (AACGM) coordinates (Baker and Wing 1989)

tailward propagation of magnetic fluctuations in the magnetosphere. Note that THEMIS-D and THEMIS-E observed the dipolarization signature again just before the electrojet reaches KTN. This may be related to the initiation of the poleward leap of the substorm current system (e.g., Wiens and Rostoker 1975; Hones 1985).

Figure 3 shows magnetic field data from RBSP-B and low-latitude ground observatories. Positive or negative excursions started almost simultaneously with the onset time at ETS-VIII shown by a vertical bar ($\sim 15:15:30$ UT). Pi2 oscillations with a period of few minutes occurred during 15:16–15:33 UT at both ground stations and RBSP-B. RBSP-B shows increases in ΔH and ΔD like a dipolarization, but their amplitude is much smaller than those observed further than the geosynchronous altitude. ASB observed a positive excursion of ΔD , indicating that the observatory was located on the western side of the current wedge. EWA observed the positive bay in ΔH . The ΔD component stays relatively at a constant level after the positive bay onset although the ΔD trend increases before the ΔH positive bay onset. Thus, the center of the large-scale current wedge was located in the postmidnight sector near the meridian at EWA

Discussion

In this section, we discuss the configuration and development of the current system during the substorm expansion phase starting at 15:15 UT on July 9, 2013. Figure 4a shows a possible distribution of FACs on the ionosphere deduced from the satellite observations. Since it is reasonable to assume the FAC is symmetric with respect to the magnetic equator, the azimuthal magnetic variation is probably opposite with respect to the magnetic equator. The azimuthal component of magnetic field variations observed in the southern hemisphere is reversely translated to the northern hemisphere and is shown as dotted green arrows. Based on the ground magnetic data at low latitudes, the MLT at QZS-1 was on the western side of the current wedge where magnetic effects of the upward FAC are dominant. If a single upward current sheet moving poleward passed through QZS-1, QZS-1 should observe an eastward magnetic field deflection after

the passing, but QZS-1 actually observed a westward deflection. The westward magnetic field deflection at QZS-1 can be explained if the downward current in the higher latitude region extends westward as shown in the FAC in Fig. 4a. In this case, there are two-layer current sheets at the meridian of QZS-1; the upward current on the equatorward side and downward current on the poleward side. The magnetic perturbation outside the current sheets is weak, and a strong westward magnetic perturbation is created near the boundary between upward and downward currents. THEMIS-D in the southern hemisphere, which observed the eastward deflection (corresponding to the westward deflection in the northern hemisphere), is also considered to be located near the boundary of the FACs. Such oblique boundary of FACs during the expansion phase has been shown by magnetic measurements from the ground magnetometers and low-altitude satellites (e.g., Iijima and Potemra 1976; Kamide et al. 1996). The double-wedge current system proposed by Gjerloev and Hoffman (2014) (Figure 8 in the paper); the higher latitude current wedge is shifted westward, also expects the same magnetic effect at QZS-1. The azimuthal magnetic field variations at the satellites in the equatorward side of the current wedge (ETS-VIII and THEMIS-E) are considered to be a temporal development of the magnitude of the upward current. The field lines at THEMIS-D and THEMIS-E were continued to become more dipole-like until currents reached to the field line near KTN and QZS-1. This means that the disrupted westward current and the related FAC at the THEMIS satellites were still large when the current system reached KTN and QZS-1. RBSP-B observed the positive D excursion in the southern hemisphere, which is opposite to the expected magnetic deflection by the upward FAC. The downward region-2 sense FAC during the substorm expansion phase (Ohtani et al. 1990) may exist just poleward of RBSP-B, although there is some ambiguity in the determination of the hemisphere of the RBSP-B as shown by a small distance from the magnetic equator of the Tsyganenko 96 model (Fig. 1b).

Although the radial distance of QZS-1 is close to the geosynchronous altitude, the onset of the magnetic fluctuation

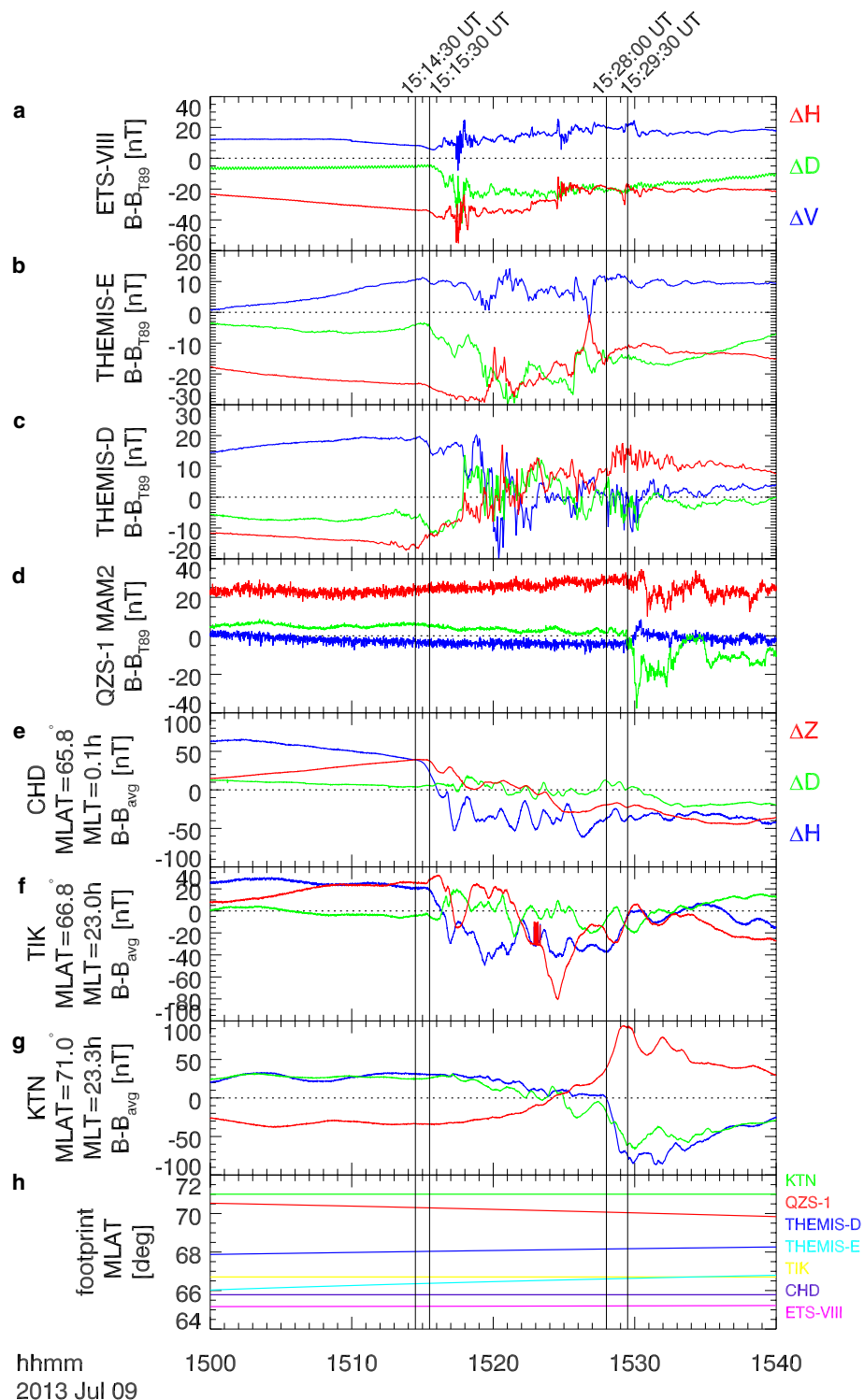
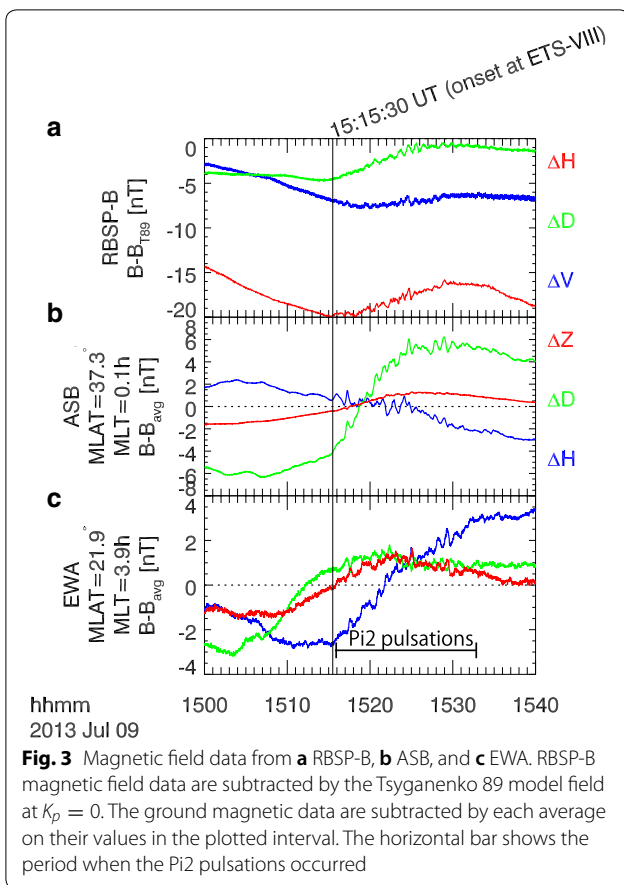
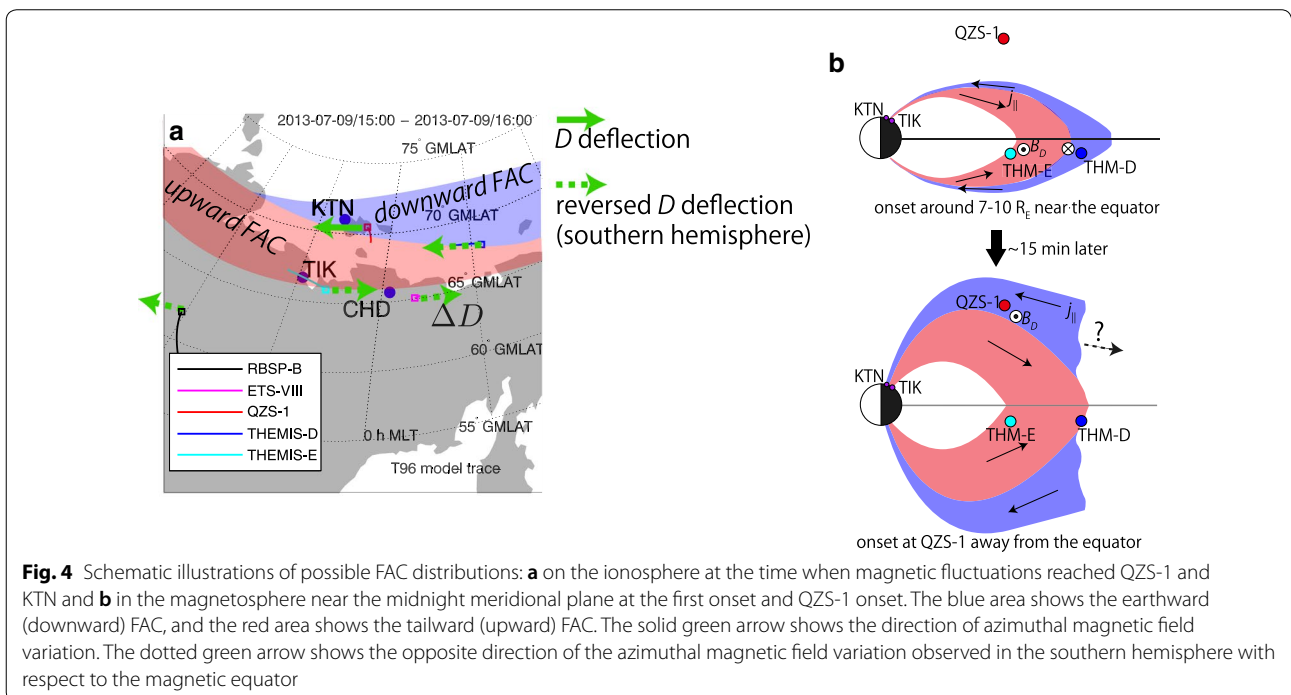


Fig. 2 Magnetic field data from **a** ETS-VIII, **b** THEMIS-E, **c** THEMIS-D, **d** QZS-1, **e** CHD, **f** TIK, and **g** KTN. The satellite magnetic field data are subtracted by the Tsyganenko 89 model field at $K_p = 0$. The ground magnetic field data are subtracted by values averaged by their values in the plotted interval. The MLTs are AACGM MLTs at 15:15 UT. (h) AACGM magnetic latitude at 100 km in altitude of ionospheric footprints of satellites and ground observatories



was observed with a large delay of ~ 15 minutes. This delay is much longer than the radial propagation time around this altitude near the equatorial plane reported by previous studies (Liou et al. 2002; Ohtani et al. 1998, 2018). Our results indicate that the propagation of the magnetic fluctuation does not only depend on the radial distance, but also strongly depends on the magnetic latitude (or distance from the magnetic equatorial plane). We discuss the delay time from the perspective of the development of the current system. Figure 4b shows a possible meridional distribution of FACs near midnight. Based on the timing consistency between ground magnetometers and satellites, the FACs were connected from the ionosphere to at least the position of QZS-1 in the magnetosphere. The speed of the poleward propagating magnetic fluctuation at the ionospheric altitude of 100 km is calculated to be $(70.5 - 68)[^\circ]/15[\text{min}] = 0.167[^\circ/\text{min}] = 310[\text{m/s}]$ by the Tsyganenko 96 model. Akasofu et al. (1966) demonstrated that the most probable range of the speed of the auroral poleward expansion was 500–600 (m/s) by analyzing auroral images from a ground-based all-sky imager. Craven and Frank (1987) demonstrated that average speeds of poleward motion were ~ 230 (m/s) and ~ 1000 (m/s) for two substorms under different conditions using auroral images from Dynamic Explorer 1. Although no auroral images were available in this longitude sector for the analyzed period, the poleward moving speed of the FAC in the magnetosphere and the westward electrojet are consistent with a typical speed of the auroral poleward expansion. Liou et al. (2002) showed that the dipolarization onset at GOES



8 geosynchronous satellite occurred at the same time as the expanding auroral bulge reached the ionospheric footprint of the satellite located on the lower-latitude side, implying the connection between the earthward propagating dipolarization and the equatorward auroral expansion. On the other hand, our study shows the connection between tailward (poleward) propagating magnetic fluctuations in the magnetosphere and the ionospheric electrojet indicated by the ground magnetometers.

We discuss the corresponding propagation speed in the equatorial plane. The farthest point of the field line (equatorial footprint) at 15:15 UT traced from QZS-1 by the Tsyganenko 96 model is the distant tail of $(X_{GSM}, Y_{GSM}, Z_{GSM}) = (-116.4, -2.8, 4.7)R_E$ and a radial distance of $116.5 R_E$. It should be noted that there can be a large error of the tracing position because the distance of the tracing is very long. Also, the field line when the FAC reach QZS-1 was probably more dipole-like, and the actual equatorial footprint expected to be closer to the earth than the model estimation. The farthest point traced from the THEMIS-D is estimated to be $(X_{GSM}, Y_{GSM}, Z_{GSM}) = (-14.9, -3.7, 4.3)R_E$ and a radial distance of $16.0 R_E$. Assuming that the FAC is along the model field line, the tailward propagating speed of FAC (or its source) in the magnetic equator between $16.0 R_E$ and $116.5 R_E$ is calculated to be $(116.5 - 16)[R_E]/15[\text{min}] = 710$ [km/s]. The speed of the tailward propagation in the equatorial plane is higher than 150–300 (km/s) at 11–22 R_E estimated by previous studies (Jacquey et al. 1991; Ohtani et al. 1992; Jacquey et al. 1993). The propagation speed at further than 15 R_E estimated by previous studies is not based on the delay time between two points, but time variations of the poloidal magnetic field. Simultaneous observations of the off-equatorial near-earth tail and a conjugate location in the down tail will make it clear where the high-latitude part of the substorm FACs comes from.

Conclusions

In this study, we examined the distribution of the magnetic fluctuations during a substorm on July 09, 2013, by simultaneous observations near and far away from the equator in the magnetosphere and conjugate ground observations. THEMIS-D, THEMIS-E, ETS-VIII, and RBSP-B were located at radial distances of about 10, 7, 6.6, and 4 R_E near the equator. QZS-1, which has a unique orbit of the quasi-zenith orbit, stays near the geosynchronous altitude far away from the magnetic equator on a timescale of the substorm. The combination of these satellites enables us to provide the information on the latitudinal distribution and development of the substorm current system in the magnetosphere.

The dipolarization first initiated at $\sim 10 R_E$ near the equator. Then, ~ 1 min later, magnetic variations were

observed near the geosynchronous orbit. At the same time, the Pi2 pulsation and magnetic bay were observed in the inner magnetosphere and ground magnetometers at low latitudes. These indicate the inward propagation from 10 R_E in the equatorial plane. We found that a large excursion of the azimuthal magnetic field was observed at a radial distance of $\sim 7 R_E$ radial distance and $\sim 30^\circ$ away from the magnetic equator with a large delay of ~ 15 minutes from the first dipolarization onset near the magnetic equator. This indicates that the onset of substorm magnetic fluctuations in the magnetosphere strongly depends on the magnetic latitude. Because the motion the fluctuation source across the field line is probably much slower than associated field-aligned propagating Alfvén waves, the source motion can be responsible for the onset timing. The large delay in the magnetosphere is consistent with the poleward motion (or leap) of the westward electrojet as the negative bay near the ionospheric footprint of the satellites. The poleward propagation speed of the magnetic fluctuation between the ionospheric footprints is consistent with a typical speed of the auroral poleward expansion. These mean that tailward (poleward) propagating magnetic fluctuations in the magnetosphere are associated with the ionospheric signature of substorms.

The timing consistency with the ground observations and the strong azimuthal fluctuation at QZS-1 indicates that the FAC poleward passed through the satellite. However, the polarity of the azimuthal magnetic field cannot be explained by passing of a single upward current sheet of a current wedge. The distribution of the azimuthal magnetic field variations in the magnetosphere suggests that the eastern side downward current extended more westward at the higher latitude part of the current wedge (Fig. 4a). Such current system expects that the strong westward magnetic variation near the boundary between upward and downward currents in the northern hemisphere as shown by the QZS-1 observation.

Abbreviations

FAC: Field-aligned current; THEMIS: Time History of Events and Macroscale Interactions during Substorms; ETS-VIII: Engineering Test Satellite VIII; QZS-1: First Quasi-Zenith Satellite; RBSP: Radiation Belt Storm Probes; MLAT: Magnetic latitude; MLT: Magnetic local time; MAGDAS/CPMN: MAGnetic Data Acquisition System/Circum-pan Pacific Magnetometer Network; AACGM: Altitude-adjusted corrected geomagnetic.

Acknowledgements

We thank all members of MAGDAS team, EMFISIS team, and FGM team. Geomagnetic fields and field line traces by the Tsyganenko models are calculated with GEOPACK routines developed by N.A. Tsyganenko and coded by H. Korth.

Availability of data and materials

Data used in this study can be obtained by contacting the following sources: Van Allen Probes Science Operation Centers located at University of Iowa (<http://emfisis.physics.uiowa.edu>) for RBSP/EMFISIS; Space Science Laboratory, University of California, Berkeley (<http://themis.ssl.berkeley.edu>) for THEMIS; Japan Aerospace Exploration Agency, Japan for ETS-VIII (contact: koga).

kiyokazu@jaxa.jp) and QZS-1 (contact: aida.mari@jaxa.jp); International Center for Space Weather Science and Education, Kyushu University for ASB, EWA, CHD, TIK, and KTN (<http://magdas.serc.kyushu-u.ac.jp>); WDC for geomagnetism, Kyoto (<http://wdc.kugi.kyoto-u.ac.jp/>) for SYM-H; OMNI web (<https://omniweb.gsfc.nasa.gov/>) for solar wind data.

Competing interests

There is no competing interests.

Funding

This study was supported in part by Grant-in-Aid for Japan Society for the Promotion of Science (JSPS) Fellows (17J00472). MN is supported by JSPS, Grant-in-Aid for Scientific Research (B) (16H04057) and Specially Promoted Research (16H06286) and by Ito Kagaku Shinkou Kai. K. H. Glassmeier, U. Auster, and W. Baumjohann for the use of FGM data provided under the lead of the Technical University of Braunschweig and with financial support through the German Ministry for Economy and Technology and the German Center for Aviation and Space (DLR) under contract 50 OC 0302.

Authors' contributions

SI analyzed data and drafted the manuscript. SI, NM, NH, MA, and HM processed and calibrated the QZS-1 data. NM, KK, and HM processed and calibrated the ETS-VIII data. AY provided MAGDAS data. NM and AY helped to interpret the results. CS and RJM made substantial contributions to the acquisition of RBSP/EMFISIS data. All authors read and approved the final manuscript.

Author details

¹ Institute for Space-Earth Environmental Research, Nagoya University, Nagoya, Japan. ² Japan Aerospace Exploration Agency, Tsukuba, Japan. ³ Institute for the Study of Earth, University of New Hampshire, New Hampshire, USA. ⁴ Solar System Exploration Division, Goddard Space Flight Center, Greenbelt, MA, USA. ⁵ Department of Earth and Planetary Sciences, Kyushu University, Fukuoka, Japan.

Received: 19 November 2019 Accepted: 23 April 2020

Published online: 07 May 2020

References

- Akasofu SI (1960) Large-scale auroral motions and polar magnetic disturbances-I a polar disturbance at about 1100 h on 23 September 1957. *J Atmos Terrest Phys* 19(1):10–25. [https://doi.org/10.1016/0021-9169\(60\)90103-3](https://doi.org/10.1016/0021-9169(60)90103-3)
- Akasofu SI, Kimball D, Meng CI (1966) Dynamics of the Aurora-V: poleward motions. *J Atmos Terrest Phys* 28(5):497–503. [https://doi.org/10.1016/0021-9169\(66\)90059-6](https://doi.org/10.1016/0021-9169(66)90059-6)
- Angelopoulos V, Sibeck D, Carlson CW, McFadden JP, Larson D, Lin RP, Bonnell JW, Mozer FS, Ergun R, Cully C, Glassmeier KH, Auster U, Roux A, LeContel O, Frey S, Phan T, Mende S, Frey H, Donovan E, Russell CT, Strangeway R, Liu J, Mann I, Rae J, Raeder J, Li X, Liu W, Singer HJ, Sergeev VA, Apatenkov S, Parks G, Fillingim M, Sigwarth J (2009) First results from the THEMIS mission. Springer, New York, pp 453–476. https://doi.org/10.1007/978-0-387-89820-9_19
- Baker KB, Wing S (1989) A new magnetic coordinate system for conjugate studies at high latitudes. *J Geophys Res* 94(A7):9139–9143. <https://doi.org/10.1029/JA094iA07p09139>
- Baumjohann W, Hesse M, Kokubun S, Mukai T, Nagai T, Petrukovich AA (1999) Substorm dipolarization and recovery. *J Geophys Res* 104(A11):24995–25000. <https://doi.org/10.1029/1999JA900282>
- Craven JD, Frank LA (1987) Latitudinal motions of the aurora during substorms. *J Geophys Res* 92(A5):4565–4573. <https://doi.org/10.1029/JA092iA05p04565>
- Cummings WD, Barfield JN, Coleman PJ (1968) Magnetospheric substorms observed at the synchronous orbit. *J Geophys Res* 73(21):6687–6698. <https://doi.org/10.1029/JA073i021p06687>
- Furuhata S, Matsumoto H, Obara T (2012) Overview of initial observation data of technical data acquisition equipments on the first Quasi-Zenith Satellite. *Trans JSASS Aerospace Tech Jpn* 10(ists28):TrA_1–TrA_5. https://doi.org/10.2322/tastj.10.Tr_1
- Gjerloev JW, Hoffman RA (2002) Currents in auroral substorms. *J Geophys Res* 107(8):1–13. <https://doi.org/10.1029/2001JA000194>
- Gjerloev JW, Hoffman RA (2014) The large-scale current system during auroral substorms. *J Geophys Res* 119(6):4591–4606. <https://doi.org/10.1002/2013JA019176>
- Hones EW (1985) The poleward leap of the auroral electrojet as seen in auroral images. *J Geophys Res* 90(A6):5333–5337. <https://doi.org/10.1029/JA090iA06p05333>
- Iijima T, Potemra TA (1976) The amplitude distribution of field-aligned currents at northern high latitudes observed by Triad. *J Geophys Res* 81(13):2165–2174. <https://doi.org/10.1029/JA081i013p02165>
- Ishijima Y, Inaba N, Matsumoto A, Terada K (2009) Design and development of the first Quasi-Zenith satellite attitude and orbit control system. In: 2009 IEEE aerospace conference, pp 1–8. <https://doi.org/10.1109/AERO.2009.4839537>
- Jacquey C, Sauvaud JA, Dandouras J (1991) Location and propagation of the magnetotail current disruption during substorm expansion: analysis and simulation of an ISEE multi-onset event. *Geophys Res Lett* 18(3):389–392. <https://doi.org/10.1029/90GL02789>
- Jacquey C, Sauvaud JA, Dandouras J, Korh A (1993) Tailward propagating cross-tail current disruption and dynamics of near-earth tail: a multi-point measurement analysis. *Geophys Res Lett* 20(10):983–986. <https://doi.org/10.1029/93GL00072>
- Kamide Y, Sun W, Akasofu SI (1996) The average ionospheric electrodynamics for the different substorm phases. *J Geophys Res* 101(A1):99–109. <https://doi.org/10.1029/95JA02990>
- Kepko L, McPherron RL, Amm O, Apatenkov S, Baumjohann W, Birn J, Lester M, Nakamura R, Pulkkinen TI, Sergeev V (2015) Substorm current wedge revisited. *Space Sci Rev* 190(1):1–46. <https://doi.org/10.1007/s11214-014-0124-9>
- Kletzing CA, Kurth WS, Acuna M, MacDowall RJ, Torbert RB, Averkamp T, Bodet D, Bounds SR, Chutter M, Connerney J, Crawford D, Dolan JS, Dvorsky R, Hospodarsky GB, Howard J, Jordanova V, Johnson RA, Kirchner DL, Mokrzycki B, Needell G, Odom J, Mark D, Pfaff R, Phillips JR, Piker CW, Remington SL, Rowland D, Santolik O, Schnurr R, Sheppard D, Smith CW, Thorne RM, Tyler J (2013) The electric and magnetic field instrument suite and integrated science (emfisis) on rbps. *Space Sci Rev* 179(1):127–181. <https://doi.org/10.1007/s11214-013-9993-6>
- Koga K, Obara T (2009) Development and measurement result of technical data acquisition equipment (TEDA) onboard ETS-VIII (in Japanese). *IEICE Tech Rep* 108(100):23–35
- Liou K, Meng CI, Lui ATY, Newell PT, Wing S (2002) Magnetic dipolarization with substorm expansion onset. *J Geophys Res* 107(A7):1–12. <https://doi.org/10.1029/2001JA000179>
- Lui ATY (1996) Current disruption in the earth's magnetosphere: observations and models. *J Geophys Res* 101(A6):13067–13088. <https://doi.org/10.1029/96JA00079>
- Lui ATY, Yoon PH, Mok C, Ryu CM (2008) Inverse cascade feature in current disruption. *J Geophys Res* 113:A1. <https://doi.org/10.1029/2008JA013521>
- Nagai T (1982) Observed magnetic substorm signatures at synchronous altitude. *J Geophys Res* 87(A6):4405–4417. <https://doi.org/10.1029/JA087iA06p04405>
- Nosé M, Takahashi K, Keika K, Kistler LM, Koga K, Koshiishi H, Matsumoto H, Shoji M, Miyashita Y, Nomura R (2014) Magnetic fluctuations embedded in dipolarization inside geosynchronous orbit and their associated selective acceleration of O⁺ ions. *J Geophys Res* 119(6):4639–4655. <https://doi.org/10.1002/2014JA019806>
- Ohtani S, Kokubun S, Nakamura R, Elphic RC, Russell CT, Baker DN (1990) Field-aligned current signatures in the near-tail region: 2. Coupling between the region 1 and the region 2 systems. *J Geophys Res* 95(A11):18913–18927. <https://doi.org/10.1029/JA095iA11p18913>
- Ohtani S, Kokubun S, Russell CT (1992) Radial expansion of the tail current disruption during substorms: A new approach to the substorm onset region. *J Geophys Res* 97(A3):3129–3136. <https://doi.org/10.1029/91JA02470>
- Ohtani S, Takahashi K, Higuchi T, Lui ATY, Spence HE, Fennell JF (1998) AMPTE/CCE-SCATHA simultaneous observations of substorm-associated magnetic fluctuations. *J Geophys Res* 103(A3):4671–4682. <https://doi.org/10.1029/97JA03239>

- Ohtani S, Motoba T, Gkioulidou M, Takahashi K, Singer HJ (2018) Spatial development of the dipolarization region in the inner magnetosphere. *J Geophys Res* 123(7):5452–5463. <https://doi.org/10.1029/2018JA025443>
- Tsyganenko N (1989) A magnetospheric magnetic field model with a warped tail current sheet. *Planet Space Sci* 37(1):5–20
- Wiens RG, Rostoker G (1975) Characteristics of the development of the westward electrojet during the expansive phase of magnetospheric substorms. *J Geophys Res* 80(16):2109–2128. <https://doi.org/10.1029/JA080i016p02109>
- Yumoto K, the MAGDAS Group (2006) MAGDAS project and its application for space weather. In: Gopalswamy N, Bhattacharya A (eds) *Solar influence*

- on the heliosphere and earth's environment: recent progress and prospects. *Wheaton, Quest Publications*, pp 399–405
- Yumoto K (2007) the MAGDAS Group Space weather activities at SERC for IHY: MAGDAS. *Bull Astr Soc India* 35:511–522

Publisher's Note

Springer Nature remains neutral with regard to jurisdictional claims in published maps and institutional affiliations.

Submit your manuscript to a SpringerOpen[®] journal and benefit from:

- ▶ Convenient online submission
- ▶ Rigorous peer review
- ▶ Open access: articles freely available online
- ▶ High visibility within the field
- ▶ Retaining the copyright to your article

Submit your next manuscript at ▶ [springeropen.com](https://www.springeropen.com)
